PB90-113218

Effects of Turbulence and Electrohydrodynamics on the Performance of Electrostatic Precipitators

Research Triangle Inst., Research Triangle Park, NC

Prepared for:

Environmental Protection Agency, Research Triangle Park, NC

1989

U.S. Department of Commerce
National Technical Information Service
NTIS

AEERL-P-587

TECHNICAL REPORT DATA
(Please read Instructions on the reverse before complet

1. REPORT NO. EPA/600/J-89/128	2.	3. PB90-113218
4. TITLE AND SUBTITLE Effects of Turbulence and Electrohydrodynamics on the Performance of Electrostatic Precipitators		5. REPORT DATE 6. PERFORMING ORGANIZATION CODE
7. AUTHOR(S) Toshiaki Yamamoto		8. PERFORMING ORGANIZATION REPORT NO.
9. PERFORMING ORGANIZATION NAME AND ADDRESS Research Triangle Institute P.O. Box 12194 Research Triangle Park, North Carolina 27709		10. PROGRAM ELEMENT NO. 11. CONTRACT/GRANT NO. EPA Cooperative Agreement CR812281
12. SPONSORING AGENCY NAME AND ADDRESS **EPA, Office of Research and Development** Air and Energy Engineering Research Laboratory **Research Triangle Park, NC 27711**		13. TYPE OF REPORT AND PERIOD COVERED Journal article; 6/87 - 5/88 14. SPONSORING AGENCY CODE **EPA/600/13**

15. SUPPLEMENTARY NOTES AEERL project officer is Leslie E. Sparks, Mail Drop 54, 919/541-2458. Journal of Electrostatics, 22 (1989) 11-22.

16. ABSTRACT The article discusses numerical simulations of the turbulent diffusion equation coupled with electrohydrodynamics (EHD), carried out for plate-plate and wire-plate ESPs. Local particle concentration profiles and fractional collection efficiencies were evaluated as a function of three dimensionless parameters: the electric Peclet number, the EHD number, and the reduced particle migration velocity. The collection efficiency for the wire-plate ESP is significantly lower than for the plate-plate ESP. For the wire-plate ESP, when the turbulent diffusion coefficient is less than 0.001 sq m/s, collection efficiency is not affected by any turbulence or EHD level. However, when the turbulent diffusion coefficient exceeds this critical value, collection efficiency drops sharply, regardless of the values of the EHD number and particle migration velocity. The critical turbulent diffusion coefficient of the plate-plate ESP is higher (0.005 sq m/s), indicating that collection efficiency is less sensitive to turbulence. The results emphasize the importance of controlling the quality of flow characteristics in the ESP.

17. KEY WORDS AND DOCUMENT ANALYSIS

a. DESCRIPTORS	b. IDENTIFIERS/OPEN ENDED TERMS	c. COSATI Field/Group
Pollution	Pollution Control	13B
Electrostatic Precipitators	Stationary Sources	13I
Turbulent Diffusion		14G
Electrohydrodynamics		20I

REPRODUCED BY
U.S. DEPARTMENT OF COMMERCE
NATIONAL TECHNICAL INFORMATION SERVICE
SPRINGFIELD, VA. 22161

18. DISTRIBUTION STATEMENT **Release to Public**	19. SECURITY CLASS *(This Report)* **Unclassified**	21. NO. OF PAGES 13
	20. SECURITY CLASS *(This page)* **Unclassified**	22. PRICE

EPA Form 2220-1 (9-73)

EPA/600/J-89/128

Journal of Electrostatics, 22 (1989) 11-22
Elsevier Science Publishers B.V., Amsterdam — Printed in The Netherlands

EFFECTS OF TURBULENCE AND ELECTROHYDRODYNAMICS ON THE PERFORMANCE OF ELECTROSTATIC PRECIPITATORS

TOSHIAKI YAMAMOTO

Research Triangle Institute, P.O. Box 12194, Research Triangle Park, NC 27709 (U.S.A.)

(Received November 24, 1987; accepted in revised form May 6, 1988)

Summary

Numerical simulations of the turbulent diffusion equation coupled with the electrohydrodynamics (EHD) are carried out for the plate-plate and wire-plate ESPs. The local particle concentration profiles and fractional collection efficiencies have been evaluated as a function of three dimensionless parameters: the electric Peclet number (Pe), the EHD number (N_{EHD}), and the reduced particle migration velocity, ϵ^*.

The collection efficiency for the wire-plate ESP is significantly lower than that for the plate-plate ESP. For the wire-plate ESP, when the turbulent diffusion coefficient is less than 1×10^{-3} m^2/s, the collection efficiency is not affected by any turbulence or EHD level. However, when the turbulent diffusion coefficient exceeds this critical value, the collection efficiency drops sharply, regardless of the values of the EHD number and particle migration velocity. The critical turbulent diffusion coefficient of the plate-plate ESP is higher, 5×10^{-3} m^2/s, indicating that the collection efficiency is less sensitive to turbulence. The results emphasize the importance of controlling the quality of flow characteristics in the ESP.

Introduction

The Deutsch equation has been used widely to predict electrostatic precipitator (ESP) performance. However, this model makes crude assumptions about the existence of uniform particle concentration profiles and, thus, complete mixing at every precipitator location. Recent theories assume the mixing to be finite [1-3]. These theories, in combination with the electrohydrodynamics (EHD), are only now evolving to the point where it is possible to model accurately the local particle concentration profile and ESP performance.

Experimental and numerical investigations of two-dimensional laminar EHD have shown the existence of circulatory cells near the collection plate [4,5]. These cells, generated by the secondary flow, modify the flow field and cause the effective cross-sectional area of the channel to decrease as the secondary flow increases. The analytical flow model was developed to take into account this variation of cross-sectional area in the gas direction.

NTIS is authorized to reproduce and sell this report. Permission for further reproduction must be obtained from the copyright owner.

© 1989 Elsevier Science Publishers B.V.

The nonuniform electric field for the wire–plate configuration that includes ionic-space-charge density is governed by Poisson and current continuity equations. The solution methods for this geometry have been well established and accepted.

In this paper, the nonuniform electric field and the EHD are incorporated into the turbulent diffusion model. The turbulent diffusion equation is derived from the particle flux within the control element and solved numerically under the following assumptions: the particles are monodispersed and precharged at the entrance, and the turbulent gas flow field has a uniform eddy diffusion throughout the domain except at the wall. The effects of turbulence and EHD on the concentration profile and collection efficiency were analyzed quantitatively by introducing three nondimensional parameters: the electric Peclet number, the EHD number, and the reduced particle migration velocity for both plate–plate and wire–plate ESPs.

Mathematical model

EHD model

In quantifying the organized secondary flow that is generated directly under the individual corona wires near the collection plate, the following assumptions were made: the flow streamlines are assumed to vary sinusoidally with the gas flow direction, and the amplitude of the displacement is assumed to decrease linearly with streamlines in the y-direction as shown in Fig. 1. With these assumptions, the EHD streamlines can be written as:

$$y(x,h) = hd + \tfrac{1}{2}(1-h)y_m\left[1+\cos\left(\frac{\pi x}{S}\right)\right] \tag{1}$$

The maximum deflection due to the secondary flow, y_m, can be estimated if N_{EHD} is defined as the ratio of the characteristic secondary flow velocity to the primary flow velocity at the ESP inlet (U_0) [4]:

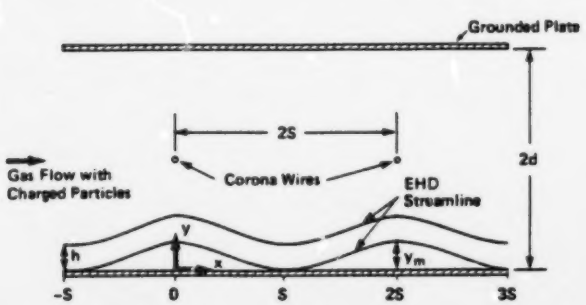

Fig. 1. Schematic of the two-wire precipitator.

$$y_m = d(0.335 \ln N_{EHD} + 0.02) \quad (2)$$

Then the variations of gas flow velocity, $u(x)$ and $v(x,h)$, are expressed as:

$$u(x) = U_0/[1 - y(x,0)/d] \quad (3)$$

$$v(x,h) = \frac{\partial y}{\partial x}\frac{\partial x}{\partial t} = \tfrac{1}{2}u(x)\ (h-1)\ \frac{\pi y_m}{S}\sin\left(\frac{\pi x}{S}\right) \quad (4)$$

Electric field calculation

Under the assumptions of steady state and no effects of magnetic field, the governing equations for the electric field and current continuity can be written as:

$$\nabla \cdot \boldsymbol{E} = \rho/\epsilon_0 \quad (5)$$

$$\boldsymbol{J} = \rho b \boldsymbol{E} \quad (6)$$

$$\boldsymbol{E} = -\nabla V \quad (7)$$

where ∇ is the vector differential operator, b is the particle mobility, ρ is the ionic space charge density, and ϵ_0 the gas permittivity (vectors are represented by boldface symbols).

Furthermore, the current density, $\boldsymbol{J}$, can be modified using eqns. (5) and (7), resulting in:

$$\rho^2 = \epsilon_0 \nabla\rho \cdot \nabla V \quad (8)$$

The boundary conditions for the potential, V, in the computational domain are: $V(0,0) = V_0$ at the wire, $V(x,d) = 0$ along the ground plate; and $E_x(0,y) = 0$, $E_x(S,y) = 0$, and $E_y(x,d) = 0$ due to the symmetry conditions, except near the wire electrode. Because details of the numerical analysis have been reported previously [6], the solution methods are omitted in this paper. The influence of the charged particles on the electric field was examined. As long as the particle space charge was below 20 $\mu C/m^3$, the electric field distribution was not significantly altered. Hence, the validity of the numerical simulation was justified by the upper limit of the particle space charge.

Turbulent diffusion model

The governing equation describing the particle concentration, n, is derived from considering the particle flux in the control volume element as shown in Fig. 2. When the particle size is in the Stokes region, the particle flux within the control element can be written as:

$$[u(x) + \mu E_x(x,y)]\frac{\partial n}{\partial x} + [v(x,y) + \mu E_y(x,y)]\frac{\partial n}{\partial y} = D\left(\frac{\partial^2 n}{\partial x^2} + \frac{\partial^2 n}{\partial y^2}\right) \quad (9)$$

where μ is the particle mobility.

Equation (9) is nondimensionalized using the following variables:

$$\begin{aligned} &\bar{x}=x/d, \quad \bar{y}=y/d, \quad \bar{n}=n/n_0, \quad \bar{u}=u/U_0, \\ &\bar{v}=v/U_0, \quad \bar{E}_x=E_x/E_0, \quad \bar{E}_y=E_y/E_0, \\ &E_0=V/d, \quad w_0=\mu E_0 \end{aligned} \tag{10}$$

Then,

$$[\bar{u}(\bar{x})/\epsilon^*+\bar{E}_x(\bar{x},\bar{y})]\frac{\partial \bar{n}}{\partial \bar{x}}+[\bar{v}(\bar{x},\bar{y})/\epsilon^*+\bar{E}_y(\bar{x},\bar{y})]\frac{\partial \bar{n}}{\partial \bar{y}}=1/Pe\left(\frac{\partial^2 \bar{n}}{\partial \bar{x}^2}+\frac{\partial^2 \bar{n}}{\partial \bar{y}^2}\right) \tag{11}$$

The particle concentration profiles and ESP efficiency are evaluated by introducing three nondimensional parameters: the electric Peclet number (Pe), which is a measure of the relative strength of external forces and diffusion on particle transport, and which is defined as $w_0 d/D$; EHD number (N_{EHD}), which is the magnitude of the secondary flow interaction; and reduced particle migration velocity (ϵ^*), which is the ratio of particle migration to primary flow velocity and which is defined as w_0/U_0.

Equation (11) is of the elliptic type and requires that all boundary conditions be specified. Because of the symmetry conditions along the centerline, only the lower half of the plane is considered (see Fig. 1). The inlet concentration, n_0, is assumed uniform. Along the centerline ($y=d$), the particle flux becomes zero because of $E_y(x,d)=0$, and $\partial n/\partial y|_d=0$. At the ground plate ($y=0$), the turbulent diffusion coefficient, D, becomes zero. At the ESP outlet, the concentration gradient in the x-direction becomes zero ($\partial n/\partial x|_{3S}=0$).

Equation (11) was solved by the Gauss–Seidel iterative method because the

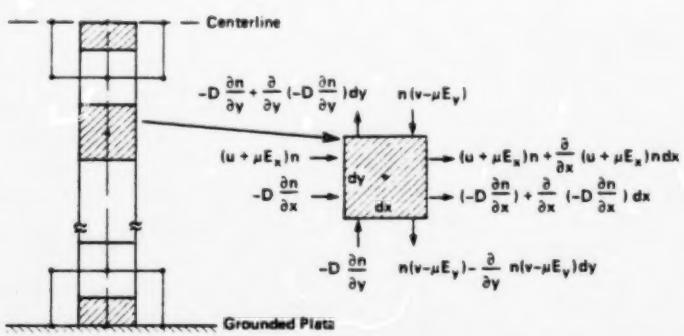

Fig. 2. Particle flux in the finite element.

successive-over-relaxation (SOR) method causes numerical instabilities. The finite difference up-wind scheme becomes as follows:

For $\bar{E}_y^*(i,j) \geq 0$:

$$\bar{n}_{i,j}\left[\bar{E}_y^*(i,j)\beta+\bar{E}_x^*(i,j)+\frac{2}{Pe(\Delta\bar{x})}(1+\beta^2)\right]$$
$$=\bar{n}_{i-1,j}\left[\bar{E}_x^*(i-1,j)+\frac{1}{Pe(\Delta\bar{x})}\right]+\bar{n}_{i+1,j}\left[\frac{1}{Pe(\Delta\bar{x})}\right]$$
$$+\beta\bar{n}_{i,j-1}\left[\frac{1}{Pe(\Delta\bar{y})}\right]+\beta\bar{n}_{i,j+1}\left[\frac{1}{Pe(\Delta\bar{y})}+\bar{E}_y^*(i,j+1)\right] \tag{12}$$

where

$$\bar{E}_y^*(i,j)=\left[\bar{E}_y(i,j)-\frac{\bar{v}_{i,j}}{\epsilon^*}\right] \quad \text{and} \quad \bar{E}_x^*(i,j)=\left[\bar{E}_x(i,j)+\frac{\bar{u}_i}{\epsilon^*}\right]$$

For $E_y^*(i,j) < 0$:

$$\bar{n}_{i,j}\left[\beta\bar{E}_y^*(i,j)+\bar{E}_x^*(i,j)+\frac{2}{Pe(\Delta\bar{x})}(1+\beta^2)\right]$$
$$=\bar{n}_{i-1,j}\left[\bar{E}_x^*(i-1,j)+\frac{1}{Pe(\Delta\bar{x})}\right]+\bar{n}_{i+1,j}\left[\frac{1}{Pe(\Delta\bar{x})}\right]$$
$$+\beta\bar{n}_{i,j-1}\left[\frac{1}{Pe(\Delta\bar{y})}+\bar{E}_y^*(i,j-1)\right]+\beta\bar{n}_{i,j+1}\left[\frac{1}{Pe(\Delta\bar{y})}\right] \tag{13}$$

Along the wall,

$$\bar{n}_{i,j}\left[2\beta\,\bar{E}_y^*(i,j)+\bar{E}_x^*(i,j)+\frac{2}{Pe(\Delta\bar{x})}(1+\beta^2)\right]$$
$$=\bar{n}_{i-1,j}\left[\bar{E}_y^*(i-1,j)+\frac{1}{Pe(\Delta\bar{x})}\right]+\bar{n}_{i+1,j}\left[\frac{1}{Pe(\Delta\bar{x})}\right]$$
$$+2\beta\,\bar{n}_{i,j+1}\left[\bar{E}_y^*(i,j+1)+\frac{1}{Pe(\Delta\bar{y})}\right] \tag{14}$$

Along the centerline,

$$\bar{n}_{i,j}\left[2\beta\bar{E}_y^*(i,j)+\bar{E}_x^*(i,j)+\frac{2}{Pe(\Delta\bar{x})}(1+\beta^2)\right]$$
$$=\bar{n}_{i-1,j}\left[\bar{E}_x^*(i-1,j)+\frac{1}{Pe(\Delta\bar{x})}\right]+\bar{n}_{i+1,j}\left[\frac{1}{Pe(\Delta\bar{x})}\right]$$
$$+2\beta\bar{n}_{i,j-1}\left[\frac{1}{Pe(\Delta\bar{x})}\right] \tag{15}$$

Results and discussion

EHD streamlines

Figure 3 shows the EHD streamlines calculated from eqns. (1) for $N_{EHD}=1.34$, which corresponds to $E_0=5.0$ kV/cm, $I=0.08$ mA/plate/m, $U_0=1.22$ m/s, $y_m=0.12d$. The corona wire locations are indicated by $x=0$ and $2S$. $\bar{u}(\bar{x})$ varies sinusoidally from 1.0 to 1.4, while $\bar{v}(\bar{x},\bar{h})$ varies from -0.20 to 0.20. Note that there are no secondary flows generated for the plate-plate ESP due to the uniform electric field.

Electric field for the wire-plate ESP

Assuming that the ESP has two corona wires with spacing equal to the duct width ($S/d=1.0$), a wire diameter $\bar{a}=a/d=0.015$, $E_0=5.0$ kV/cm, and $I=0.08$ mA/plate/m, Figs. 4a and b illustrate the x-component ($\bar{E}_x$) and y-component ($\bar{E}_y$) of the normalized field strength for various x-locations. These results are similar to the results obtained by Kihm et al. [2].

Particle concentration profile for the plate-plate ESP

Figure 5a shows the particle concentration profile as a function of $\bar{x}$ for the uniform migration velocity that corresponds to the plate-plate precipitator having an ESP length of $4S$. The computation was carried out with $\bar{u}(\bar{x},\bar{y})=1.0$. $\bar{v}(\bar{x},\bar{y})=0$, $\bar{E}_x(\bar{x},\bar{y})=0$, and $\bar{E}_y(\bar{x},\bar{y})=1.0$ The grid points used were (41×11),

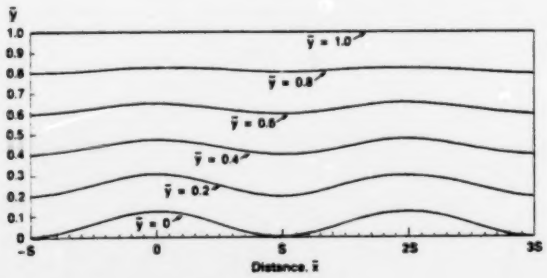

Fig. 3. EHD streamlines for $N_{EHD}=1.34$.

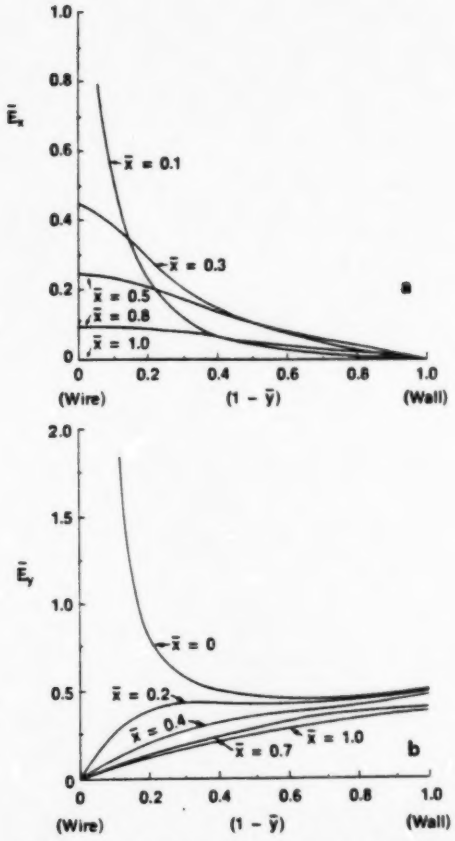

Fig. 4. Normalized field distribution; (a) x-component ($\bar{E}_x$); (b) y-component ($\bar{E}_y$).

which resulted in $\beta = 1.0$ for this case. The particle concentrations were plotted in six locations: $\bar{y} = 0$, 0.3, 0.5, 0.7, 0.9, and 1.0 for the typical parameter values of $\epsilon^* = 0.1$, $Pe = 100$ (or $D = 0.37 \times 10^{-4}$ m^2/s). As expected, it was seen that the concentration near the wall gradually decreased along the flow direction ($\bar{x}$), while the particle concentrations near the centerline remained unchanged all the way to the outlet. This concentration profile agreed well with the experimental results obtained by Leonard et al. [1].

Figure 5b shows the results for the same conditions as in Fig. 5a except for higher turbulence ($Pe = 20$ or $D = 0.18 \times 10^{-3}$ m^2/s). The particle concentrations are increased near the collection plate and flattened out over the entire domain, due to increased turbulent diffusion. The resulting fractional collection efficiency, η, is slightly reduced from 39.9 to 39.6 percent as Pe changes from 100 to 20.

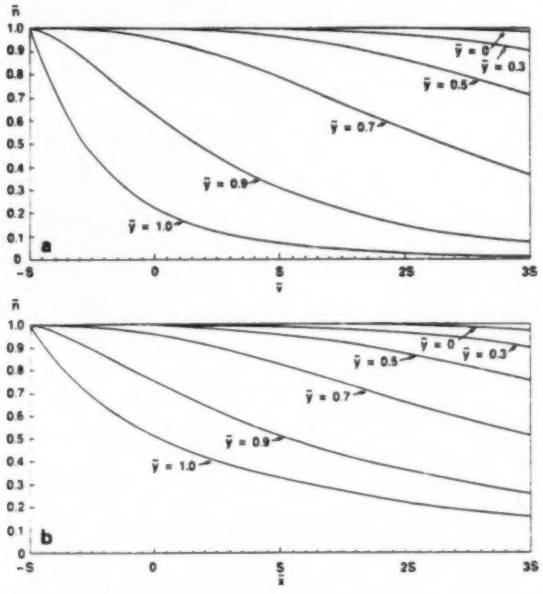

Fig. 5. Normalized particle concentration profiles for the plate-plate ESP; (a) $\epsilon^* = 0.1$, $Pe = 100$, $N_{EHD} = 0$, $\eta = 39.9\%$; (b) $\epsilon^* = 0.1$, $Pe = 20$, $N_{EHD} = 0$, $\eta = 39.6\%$.

Particle concentration profile for the wire-plate ESP

When $\bar{u}(\bar{x},\bar{y}) = 1.0$, $\bar{v}(\bar{x},\bar{y}) = 0$, and $\bar{E}_x(\bar{x},\bar{y})$ and $\bar{E}_y(\bar{x},\bar{y})$ are the space-charge-free Laplace solutions, the governing equations are reduced to the model of Kihm et al. [2]. Figures 6a–c show the normalized concentration profiles for $\epsilon^* = 0.1$ and $N_{EHD} = 0$, for various values of Pe. When the flow is laminar ($Pe = 100$ or $D = 0.37 \times 10^{-4}\ m^2/s$), as shown in Fig. 6a, the particle concentration increases near the centerline of the ESP because of the repulsive field strength $\bar{E}_x$ in the negative direction and no contribution by $\bar{E}_y$. This results in a concentration peak around the corona wire. The particle concentration drops sharply just after the corona wire due to the high field strength, $\bar{E}_y$, and gradually increases when approaching the second wire, due to particle diffusion, while the particle concentration for $0 \leqslant \bar{y} \leqslant 0.7$ remains the same and slowly decreases in the $\bar{x}$-direction. These phenomena have been observed in many smoke tests. The concentration profile generally agrees well with those found by Kihm et al. [2] except that the concentration peaks that were found were not present in their results.

Figure 6b shows the results for the same parameters as in Fig. 6a except for higher turbulent diffusion ($Pe = 10$ or $D = 0.37 \times 10^{-3}\ m^2/s$). After passing the corona wire, the particle concentration profile near the centerline increases

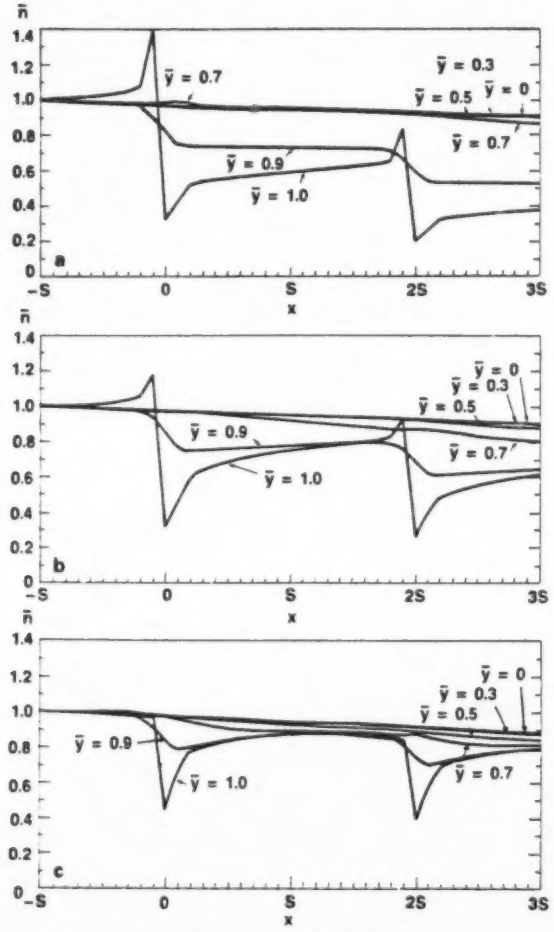

Fig. 6. Normalized particle concentration profiles for the wire-plate ESP; (a) $\epsilon^* = 0.1$, $Pe = 100$, $N_{EHD} = 0$, $\eta = 17.1\%$; (b) $\epsilon^* = 0.1$, $Pe = 10$, $N_{EHD} = 0$, $\eta = 17.0\%$; (c) $\epsilon^* = 0.1$, $Pe = 2$, $N_{EHD} = 0$, $\eta = 11.6\%$.

faster as a result of higher turbulent diffusion. When the flow becomes highly turbulent ($Pe = 2$ or $D = 1.83 \times 10^{-3}$ cm^2/s), the concentration peak essentially disappears, as shown in Fig. 6c, and the concentration profile becomes uniform due to strong turbulent diffusion at the ESP outlet.

When the EHD effect is taken into account ($N_{EHD} = 1.34$ or $y_m = 0.2d$), the particle concentration profile for $Pe = 100$ (or $D = 0.37 \times 10^{-4}$ m^2/s) and $\epsilon^* = 0.1$ are shown in Fig. 7a. As can be seen from the figure, the concentration profile

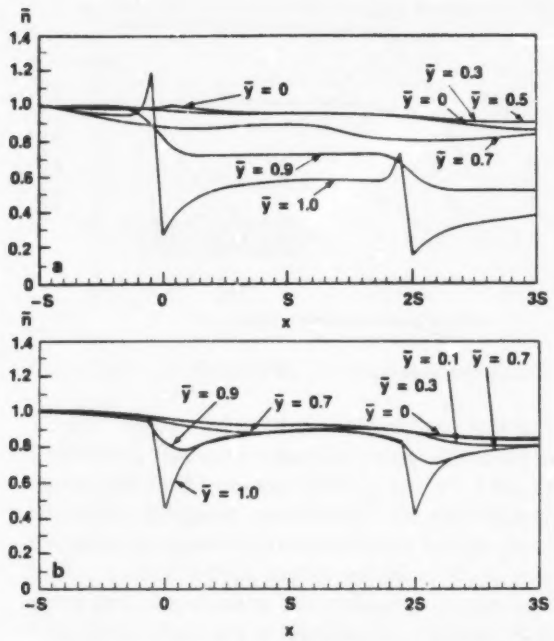

Fig. 7. Normalized particle concentration profiles for the wire-plate ESP; (a) $\epsilon^*=0.1$, $Pe=100$, $N_{EHD}=1.34$, $\eta=16.4\%$; (b) $\epsilon^*=0.1$, $Pe=2$, $N_{EHD}=1.34$, $\eta=16.6\%$.

becomes more wavy in the x-direction compared to the non-EHD case (Fig. 6a). The concentration peak becomes smaller because the primary velocity increases due to the secondary flow when approaching the wire electrode. As the turbulence further increases ($Pe=2$, or $D=0.18\times10^{-2}\,m^2/s$), the concentration profile becomes uniform and similar to the non-EHD case shown in Fig. 6c. This indicates that the turbulence dominates over the EHD or, in other words, the EHD effect disappears at high turbulence.

It should be noted that the diffusion approach, which includes the effect of the negative particle migration due to the concentration gradient, results in uniform concentration at high turbulence. As the value of D approaches infinity, the particle diffusion cancels out the particle migration, resulting in extremely low collection efficiency. On the other hand, the Deutsch assumption, which should be distinguished from the diffusion approach, simply assumes uniform concentration throughout the channel. Therefore, the collection efficiency is expected to be lower using the diffusion approach with high turbulence than that determined with the Deutsch assumption.

Figure 8 shows the fractional collection efficiency for the wire–plate ESP and plate–plate ESP. In the case of the wire–plate ESP, for values of D below

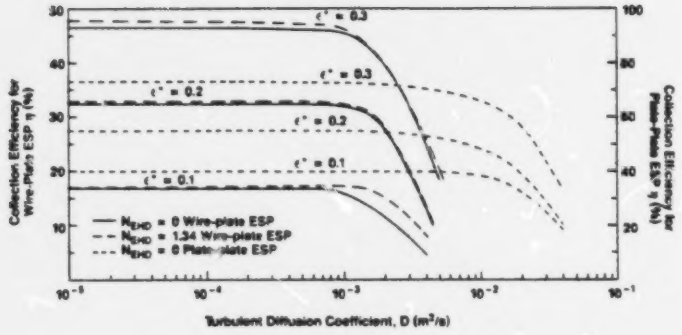
Collection Efficiency for Wire-Plate ESP η (%)
Collection Efficiency for Plate-Plate ESP η (%)
Turbulent Diffusion Coefficient, D (m²/s)
ε* = 0.3
ε* = 0.2
ε* = 0.1
N_EHD = 0 Wire-plate ESP
N_EHD = 1.34 Wire-plate ESP
N_EHD = 0 Plate-plate ESP

Fig. 8. Collection efficiency for both wire-plate and plate-plate ESPs.

1×10^{-3} m^2/s, the collection efficiency, η, is not affected by any turbulence or EHD level. However, when the value of D exceeds 1×10^{-3} m^2/s, η drops sharply regardless of the values of N_{EHD} and ϵ^*. This value of D is called "the critical turbulent diffusion coefficient" for the wire-plate ESP. Because numerical instabilities have been encountered for low Pe numbers (high turbulence), the higher η obtained for higher values of N_{EHD} may well be within the numerical error and therefore is inconclusive. In the case of the plate-plate ESP, the collection efficiency is significantly higher than for the wire-plate ESP. The critical turbulent diffusion coefficient increases to approximately 5×10^{-3} m^2/s. This indicates that η of the plate-plate ESP is less sensitive to the turbulence compared to that of the wire-plate ESP. It is also noted that η does not increase linearly with increasing ϵ^*.

The role of the EHD is to generate their circulatory cell near the plate and also to increase the turbulence, which is especially significant for the negative corona. It is clear from the present study that one of the most important considerations in designing the ESP is to reduce the turbulence level to less than the critical turbulent diffusion coefficient, so that the collection efficiency is dependent on particle migration and independent of turbulent or EHD effects.

References

1 G.L. Leonard, M. Mitchner and S.A. Self, Experimental study of the effect of turbulent diffusion on precipitator efficiency, J. Aerosol Sci., 13 (1982) 271-284.

2 K.D. Kihm, M. Mitchner and S.A. Self, Comparison of wire-plate and plate-plate electrostatic precipitators in turbulent flow, HTGL Report No. J-8, High Temperature Gasdynamics Laboratory, Mechanical Engineering Department, Stanford University, Stanford, CA, March 1985.

3 T. Yamamoto and L.E. Sparks, Effect of turbulent electrohydrodynamics on electrostatic precipitator efficiency, in: AIAA/ASME Fourth Fluid Mechanics, Gas Solid Flows, Plasma Dynamics and Lasers Conference, Atlanta, GA, May 1986, Vol. 35, pp. 35-39.

4 T. Yamamoto and H.R. Velkoff, Electrohydrodynamics in an electrostatic precipitator, J. Fluid Mech., 108 (1981) 1-18.
5 T. Yamamoto and L.E. Sparks, Numerical simulation of three-dimensional tuft corona and electrohydrodynamics, IEEE Trans. Ind. Appl., IA-22(5) (September/October 1986) 880-885.
6 T. Yamamoto, S. Nakamura and H.R. Velkoff, Numerical study of secondary flow interaction in an electrostatic precipitator, in: Innovative Numerical Analysis for Applied Engineering Science, University Press of Virginia, Charlottesville, VA, 1980, pp. 3-12.

NOTICE

This document has been reviewed in accordance with U.S. Environmental Protection Agency policy and approved for publication. Mention of trade names or commercial products does not constitute endorsement or recommendation for use.

This article documents research that was conducted under the auspices of the U.S. Environmental Protection Agency (USEPA). As an arm of the government, the USEPA has a paid up, non-exclusive, irrevocable, worldwide license to reproduce, prepare derivative works, and distribute to the public all of the material contained herein, and to grant others acting on its behalf the right to do so. The USEPA grants to the National Technical Information Service, Department of Commerce, the right to act as its agent in the distribution of this material.

PB90-113218

Effects of Turbulence and Electrohydrodynamics on the Performance of Electrostatic Precipitators

Research Triangle Inst., Research Triangle Park, NC

Prepared for:

Environmental Protection Agency, Research Triangle Park, NC

1989

U.S. Department of Commerce
National Technical Information Service
NTIS

AEERL-P-587

TECHNICAL REPORT DATA
(Please read Instructions on the reverse before complet

1. REPORT NO. EPA/600/J-89/128	2.	3. PB90-113218
4. TITLE AND SUBTITLE Effects of Turbulence and Electrohydrodynamics on the Performance of Electrostatic Precipitators		5. REPORT DATE 6. PERFORMING ORGANIZATION CODE
7. AUTHOR(S) Toshiaki Yamamoto		8. PERFORMING ORGANIZATION REPORT NO.
9. PERFORMING ORGANIZATION NAME AND ADDRESS Research Triangle Institute P.O. Box 12194 Research Triangle Park, North Carolina 27709		10. PROGRAM ELEMENT NO. 11. CONTRACT/GRANT NO. EPA Cooperative Agreement CR812281
12. SPONSORING AGENCY NAME AND ADDRESS **EPA, Office of Research and Development** Air and Energy Engineering Research Laboratory **Research Triangle Park, NC 27711**		13. TYPE OF REPORT AND PERIOD COVERED Journal article; 6/87 - 5/88 14. SPONSORING AGENCY CODE **EPA/600/13**

15. SUPPLEMENTARY NOTES AEERL project officer is Leslie E. Sparks, Mail Drop 54, 919/541-2458. Journal of Electrostatics, 22 (1989) 11-22.

16. ABSTRACT The article discusses numerical simulations of the turbulent diffusion equation coupled with electrohydrodynamics (EHD), carried out for plate-plate and wire-plate ESPs. Local particle concentration profiles and fractional collection efficiencies were evaluated as a function of three dimensionless parameters: the electric Peclet number, the EHD number, and the reduced particle migration velocity. The collection efficiency for the wire-plate ESP is significantly lower than for the plate-plate ESP. For the wire-plate ESP, when the turbulent diffusion coefficient is less than 0.001 sq m/s, collection efficiency is not affected by any turbulence or EHD level. However, when the turbulent diffusion coefficient exceeds this critical value, collection efficiency drops sharply, regardless of the values of the EHD number and particle migration velocity. The critical turbulent diffusion coefficient of the plate-plate ESP is higher (0.005 sq m/s), indicating that collection efficiency is less sensitive to turbulence. The results emphasize the importance of controlling the quality of flow characteristics in the ESP.

17. KEY WORDS AND DOCUMENT ANALYSIS

a. DESCRIPTORS	b. IDENTIFIERS/OPEN ENDED TERMS	c. COSATI Field/Group
Pollution	Pollution Control	13B
Electrostatic Precipitators	Stationary Sources	13I
Turbulent Diffusion		14G
Electrohydrodynamics		20I

REPRODUCED BY
U.S. DEPARTMENT OF COMMERCE
NATIONAL TECHNICAL INFORMATION SERVICE
SPRINGFIELD, VA. 22161

18. DISTRIBUTION STATEMENT **Release to Public**	19. SECURITY CLASS *(This Report)* **Unclassified** 20. SECURITY CLASS *(This page)* **Unclassified**	21. NO. OF PAGES 13 22. PRICE

EPA Form 2220-1 (9-73)

EPA/600/J-89/128

Journal of Electrostatics, 22 (1989) 11-22
Elsevier Science Publishers B.V., Amsterdam — Printed in The Netherlands

EFFECTS OF TURBULENCE AND ELECTROHYDRODYNAMICS ON THE PERFORMANCE OF ELECTROSTATIC PRECIPITATORS

TOSHIAKI YAMAMOTO

Research Triangle Institute, P.O. Box 12194, Research Triangle Park, NC 27709 (U.S.A.)

(Received November 24, 1987; accepted in revised form May 6, 1988)

Summary

Numerical simulations of the turbulent diffusion equation coupled with the electrohydrodynamics (EHD) are carried out for the plate-plate and wire-plate ESPs. The local particle concentration profiles and fractional collection efficiencies have been evaluated as a function of three dimensionless parameters: the electric Peclet number (Pe), the EHD number (N_{EHD}), and the reduced particle migration velocity, ϵ^*.

The collection efficiency for the wire-plate ESP is significantly lower than that for the plate-plate ESP. For the wire-plate ESP, when the turbulent diffusion coefficient is less than 1×10^{-3} m^2/s, the collection efficiency is not affected by any turbulence or EHD level. However, when the turbulent diffusion coefficient exceeds this critical value, the collection efficiency drops sharply, regardless of the values of the EHD number and particle migration velocity. The critical turbulent diffusion coefficient of the plate-plate ESP is higher, 5×10^{-3} m^2/s, indicating that the collection efficiency is less sensitive to turbulence. The results emphasize the importance of controlling the quality of flow characteristics in the ESP.

Introduction

The Deutsch equation has been used widely to predict electrostatic precipitator (ESP) performance. However, this model makes crude assumptions about the existence of uniform particle concentration profiles and, thus, complete mixing at every precipitator location. Recent theories assume the mixing to be finite [1-3]. These theories, in combination with the electrohydrodynamics (EHD), are only now evolving to the point where it is possible to model accurately the local particle concentration profile and ESP performance.

Experimental and numerical investigations of two-dimensional laminar EHD have shown the existence of circulatory cells near the collection plate [4,5]. These cells, generated by the secondary flow, modify the flow field and cause the effective cross-sectional area of the channel to decrease as the secondary flow increases. The analytical flow model was developed to take into account this variation of cross-sectional area in the gas direction.

NTIS is authorized to reproduce and sell this report. Permission for further reproduction must be obtained from the copyright owner.

© 1989 Elsevier Science Publishers B.V.

The nonuniform electric field for the wire–plate configuration that includes ionic-space-charge density is governed by Poisson and current continuity equations. The solution methods for this geometry have been well established and accepted.

In this paper, the nonuniform electric field and the EHD are incorporated into the turbulent diffusion model. The turbulent diffusion equation is derived from the particle flux within the control element and solved numerically under the following assumptions: the particles are monodispersed and precharged at the entrance, and the turbulent gas flow field has a uniform eddy diffusion throughout the domain except at the wall. The effects of turbulence and EHD on the concentration profile and collection efficiency were analyzed quantitatively by introducing three nondimensional parameters: the electric Peclet number, the EHD number, and the reduced particle migration velocity for both plate–plate and wire–plate ESPs.

Mathematical model

EHD model

In quantifying the organized secondary flow that is generated directly under the individual corona wires near the collection plate, the following assumptions were made: the flow streamlines are assumed to vary sinusoidally with the gas flow direction, and the amplitude of the displacement is assumed to decrease linearly with streamlines in the y-direction as shown in Fig. 1. With these assumptions, the EHD streamlines can be written as:

$$y(x,h) = hd + \tfrac{1}{2}(1-h)y_m\left[1+\cos\left(\frac{\pi x}{S}\right)\right] \tag{1}$$

The maximum deflection due to the secondary flow, y_m, can be estimated if N_{EHD} is defined as the ratio of the characteristic secondary flow velocity to the primary flow velocity at the ESP inlet (U_0) [4]:

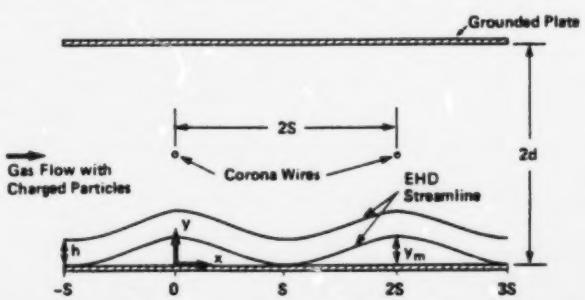

Fig. 1. Schematic of the two-wire precipitator.

$$y_m = d(0.335 \ln N_{EHD} + 0.02) \tag{2}$$

Then the variations of gas flow velocity, $u(x)$ and $v(x,h)$, are expressed as:

$$u(x) = U_0/[1 - y(x,0)/d] \tag{3}$$

$$v(x,h) = \frac{\partial y}{\partial x}\frac{\partial x}{\partial t} = \tfrac{1}{2}u(x)\ (h-1)\ \frac{\pi y_m}{S}\sin\left(\frac{\pi x}{S}\right) \tag{4}$$

Electric field calculation

Under the assumptions of steady state and no effects of magnetic field, the governing equations for the electric field and current continuity can be written as:

$$\nabla \cdot \boldsymbol{E} = \rho/\epsilon_0 \tag{5}$$

$$\boldsymbol{J} = \rho b \boldsymbol{E} \tag{6}$$

$$\boldsymbol{E} = -\nabla V \tag{7}$$

where ∇ is the vector differential operator, b is the particle mobility, ρ is the ionic space charge density, and ϵ_0 the gas permittivity (vectors are represented by boldface symbols).

Furthermore, the current density, $\boldsymbol{J}$, can be modified using eqns. (5) and (7), resulting in:

$$\rho^2 = \epsilon_0 \nabla\rho \cdot \nabla V \tag{8}$$

The boundary conditions for the potential, V, in the computational domain are: $V(0,0) = V_0$ at the wire, $V(x,d) = 0$ along the ground plate; and $E_x(0,y) = 0$, $E_x(S,y) = 0$, and $E_y(x,d) = 0$ due to the symmetry conditions, except near the wire electrode. Because details of the numerical analysis have been reported previously [6], the solution methods are omitted in this paper. The influence of the charged particles on the electric field was examined. As long as the particle space charge was below 20 $\mu C/m^3$, the electric field distribution was not significantly altered. Hence, the validity of the numerical simulation was justified by the upper limit of the particle space charge.

Turbulent diffusion model

The governing equation describing the particle concentration, n, is derived from considering the particle flux in the control volume element as shown in Fig. 2. When the particle size is in the Stokes region, the particle flux within the control element can be written as:

$$[u(x) + \mu E_x(x,y)]\frac{\partial n}{\partial x} + [v(x,y) + \mu E_y(x,y)]\frac{\partial n}{\partial y} = D\left(\frac{\partial^2 n}{\partial x^2} + \frac{\partial^2 n}{\partial y^2}\right) \tag{9}$$

where μ is the particle mobility.

Equation (9) is nondimensionalized using the following variables:

$$\begin{aligned} &\bar{x}=x/d, \quad \bar{y}=y/d, \quad \bar{n}=n/n_0, \quad \bar{u}=u/U_0, \\ &\bar{v}=v/U_0, \quad \bar{E}_x=E_x/E_0, \quad \bar{E}_y=E_y/E_0, \\ &E_0=V/d, \quad w_0=\mu E_0 \end{aligned} \tag{10}$$

Then,

$$[\bar{u}(\bar{x})/\epsilon^*+\bar{E}_x(\bar{x},\bar{y})]\frac{\partial \bar{n}}{\partial \bar{x}}+[\bar{v}(\bar{x},\bar{y})/\epsilon^*+\bar{E}_y(\bar{x},\bar{y})]\frac{\partial \bar{n}}{\partial \bar{y}}=1/Pe\left(\frac{\partial^2 \bar{n}}{\partial \bar{x}^2}+\frac{\partial^2 \bar{n}}{\partial \bar{y}^2}\right) \tag{11}$$

The particle concentration profiles and ESP efficiency are evaluated by introducing three nondimensional parameters: the electric Peclet number (Pe), which is a measure of the relative strength of external forces and diffusion on particle transport, and which is defined as $w_0 d/D$; EHD number (N_{EHD}), which is the magnitude of the secondary flow interaction; and reduced particle migration velocity (ϵ^*), which is the ratio of particle migration to primary flow velocity and which is defined as w_0/U_0.

Equation (11) is of the elliptic type and requires that all boundary conditions be specified. Because of the symmetry conditions along the centerline, only the lower half of the plane is considered (see Fig. 1). The inlet concentration, n_0, is assumed uniform. Along the centerline ($y=d$), the particle flux becomes zero because of $E_y(x,d)=0$, and $\partial n/\partial y|_d=0$. At the ground plate ($y=0$), the turbulent diffusion coefficient, D, becomes zero. At the ESP outlet, the concentration gradient in the x-direction becomes zero ($\partial n/\partial x|_{3S}=0$).

Equation (11) was solved by the Gauss–Seidel iterative method because the

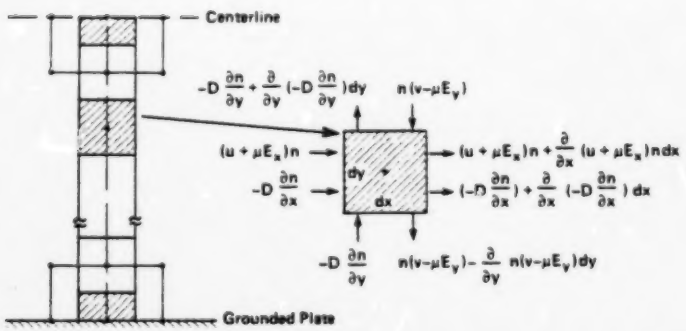

Fig. 2. Particle flux in the finite element.

successive-over-relaxation (SOR) method causes numerical instabilities. The finite difference up-wind scheme becomes as follows:

For $\bar{E}_y^*(i,j) \geq 0$:

$$\bar{n}_{i,j}\left[\bar{E}_y^*(i,j)\beta+\bar{E}_x^*(i,j)+\frac{2}{Pe(\Delta\bar{x})}(1+\beta^2)\right]$$
$$=\bar{n}_{i-1,j}\left[\bar{E}_x^*(i-1,j)+\frac{1}{Pe(\Delta\bar{x})}\right]+\bar{n}_{i+1,j}\left[\frac{1}{Pe(\Delta\bar{x})}\right]$$
$$+\beta\bar{n}_{i,j-1}\left[\frac{1}{Pe(\Delta\bar{y})}\right]+\beta\bar{n}_{i,j+1}\left[\frac{1}{Pe(\Delta\bar{y})}+\bar{E}_y^*(i,j+1)\right] \tag{12}$$

where

$$\bar{E}_y^*(i,j)=\left[\bar{E}_y(i,j)-\frac{\bar{v}_{i,j}}{\epsilon^*}\right] \quad \text{and} \quad \bar{E}_x^*(i,j)=\left[\bar{E}_x(i,j)+\frac{\bar{u}_i}{\epsilon^*}\right]$$

For $E_y^*(i,j)<0$:

$$\bar{n}_{i,j}\left[\beta\bar{E}_y^*(i,j)+\bar{E}_x^*(i,j)+\frac{2}{Pe(\Delta\bar{x})}(1+\beta^2)\right]$$
$$=\bar{n}_{i-1,j}\left[\bar{E}_x^*(i-1,j)+\frac{1}{Pe(\Delta\bar{x})}\right]+\bar{n}_{i+1,j}\left[\frac{1}{Pe(\Delta\bar{x})}\right]$$
$$+\beta\bar{n}_{i,j-1}\left[\frac{1}{Pe(\Delta\bar{y})}+\bar{E}_y^*(i,j-1)\right]+\beta\bar{n}_{i,j+1}\left[\frac{1}{Pe(\Delta\bar{y})}\right] \tag{13}$$

Along the wall,

$$\bar{n}_{i,j}\left[2\beta\,\bar{E}_y^*(i,j)+\bar{E}_x^*(i,j)+\frac{2}{Pe(\Delta\bar{x})}(1+\beta^2)\right]$$
$$=\bar{n}_{i-1,j}\left[\bar{E}_y^*(i-1,j)+\frac{1}{Pe(\Delta\bar{x})}\right]+\bar{n}_{i+1,j}\left[\frac{1}{Pe(\Delta\bar{x})}\right]$$
$$+2\beta\,\bar{n}_{i,j+1}\left[\bar{E}_y^*(i,j+1)+\frac{1}{Pe(\Delta\bar{y})}\right] \tag{14}$$

Along the centerline,

$$\bar{n}_{i,j}\left[2\beta\bar{E}_y^*(i,j)+\bar{E}_x^*(i,j)+\frac{2}{Pe(\Delta\bar{x})}(1+\beta^2)\right]$$
$$=\bar{n}_{i-1,j}\left[\bar{E}_x^*(i-1,j)+\frac{1}{Pe(\Delta\bar{x})}\right]+\bar{n}_{i+1,j}\left[\frac{1}{Pe(\Delta\bar{x})}\right]$$
$$+2\beta\bar{n}_{i,j-1}\left[\frac{1}{Pe(\Delta\bar{x})}\right] \tag{15}$$

Results and discussion

EHD streamlines

Figure 3 shows the EHD streamlines calculated from eqns. (1) for $N_{EHD}=1.34$, which corresponds to $E_0=5.0$ kV/cm, $I=0.08$ mA/plate/m, $U_0=1.22$ m/s, $y_m=0.12d$. The corona wire locations are indicated by $x=0$ and $2S$. $\bar{u}(\bar{x})$ varies sinusoidally from 1.0 to 1.4, while $\bar{v}(\bar{x},\bar{h})$ varies from -0.20 to 0.20. Note that there are no secondary flows generated for the plate–plate ESP due to the uniform electric field.

Electric field for the wire-plate ESP

Assuming that the ESP has two corona wires with spacing equal to the duct width ($S/d=1.0$), a wire diameter $\bar{a}=a/d=0.015$, $E_0=5.0$ kV/cm, and $I=0.08$ mA/plate/m, Figs. 4a and b illustrate the x-component ($\bar{E}_x$) and y-component ($\bar{E}_y$) of the normalized field strength for various x-locations. These results are similar to the results obtained by Kihm et al. [2].

Particle concentration profile for the plate-plate ESP

Figure 5a shows the particle concentration profile as a function of $\bar{x}$ for the uniform migration velocity that corresponds to the plate–plate precipitator having an ESP length of $4S$. The computation was carried out with $\bar{u}(\bar{x},\bar{y})=1.0$, $\bar{v}(\bar{x},\bar{y})=0$, $\bar{E}_x(\bar{x},\bar{y})=0$, and $\bar{E}_y(\bar{x},\bar{y})=1.0$ The grid points used were (41×11),

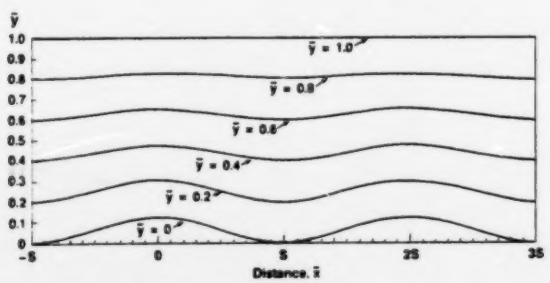

Fig. 3. EHD streamlines for $N_{EHD}=1.34$.

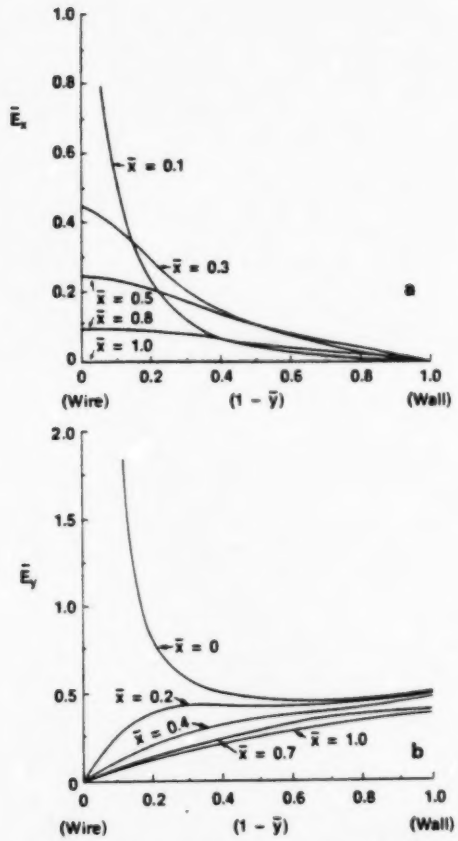

Fig. 4. Normalized field distribution; (a) x-component ($\bar{E}_x$); (b) y-component ($\bar{E}_y$).

which resulted in $\beta = 1.0$ for this case. The particle concentrations were plotted in six locations: $\bar{y} = 0$, 0.3, 0.5, 0.7, 0.9, and 1.0 for the typical parameter values of $\epsilon^* = 0.1$, $Pe = 100$ (or $D = 0.37 \times 10^{-4}$ m^2/s). As expected, it was seen that the concentration near the wall gradually decreased along the flow direction ($\bar{x}$), while the particle concentrations near the centerline remained unchanged all the way to the outlet. This concentration profile agreed well with the experimental results obtained by Leonard et al. [1].

Figure 5b shows the results for the same conditions as in Fig. 5a except for higher turbulence ($Pe = 20$ or $D = 0.18 \times 10^{-3}$ m^2/s). The particle concentrations are increased near the collection plate and flattened out over the entire domain, due to increased turbulent diffusion. The resulting fractional collection efficiency, η, is slightly reduced from 39.9 to 39.6 percent as Pe changes from 100 to 20.

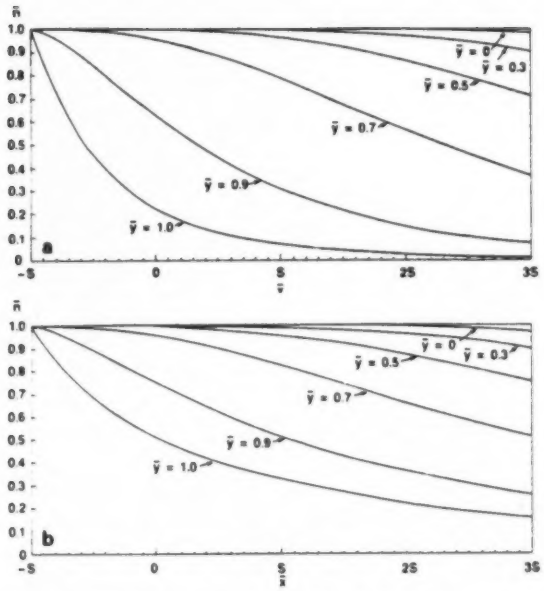

Fig. 5. Normalized particle concentration profiles for the plate-plate ESP; (a) $\epsilon^* = 0.1$, $Pe = 100$, $N_{EHD} = 0$, $\eta = 39.9\%$; (b) $\epsilon^* = 0.1$, $Pe = 20$, $N_{EHD} = 0$, $\eta = 39.6\%$.

Particle concentration profile for the wire-plate ESP

When $\bar{u}(\bar{x}\bar{y}) = 1.0$, $\bar{v}(\bar{x}\bar{y}) = 0$, and $\bar{E}_x(\bar{x}\bar{y})$ and $\bar{E}_y(\bar{x}\bar{y})$ are the space-charge-free Laplace solutions, the governing equations are reduced to the model of Kihm et al. [2]. Figures 6a–c show the normalized concentration profiles for $\epsilon^* = 0.1$ and $N_{EHD} = 0$, for various values of Pe. When the flow is laminar ($Pe = 100$ or $D = 0.37 \times 10^{-4}\ m^2/s$), as shown in Fig. 6a, the particle concentration increases near the centerline of the ESP because of the repulsive field strength $\bar{E}_x$ in the negative direction and no contribution by $\bar{E}_y$. This results in a concentration peak around the corona wire. The particle concentration drops sharply just after the corona wire due to the high field strength, $\bar{E}_y$, and gradually increases when approaching the second wire, due to particle diffusion, while the particle concentration for $0 \leqslant \bar{y} \leqslant 0.7$ remains the same and slowly decreases in the $\bar{x}$-direction. These phenomena have been observed in many smoke tests. The concentration profile generally agrees well with those found by Kihm et al. [2] except that the concentration peaks that were found were not present in their results.

Figure 6b shows the results for the same parameters as in Fig. 6a except for higher turbulent diffusion ($Pe = 10$ or $D = 0.37 \times 10^{-3}\ m^2/s$). After passing the corona wire, the particle concentration profile near the centerline increases

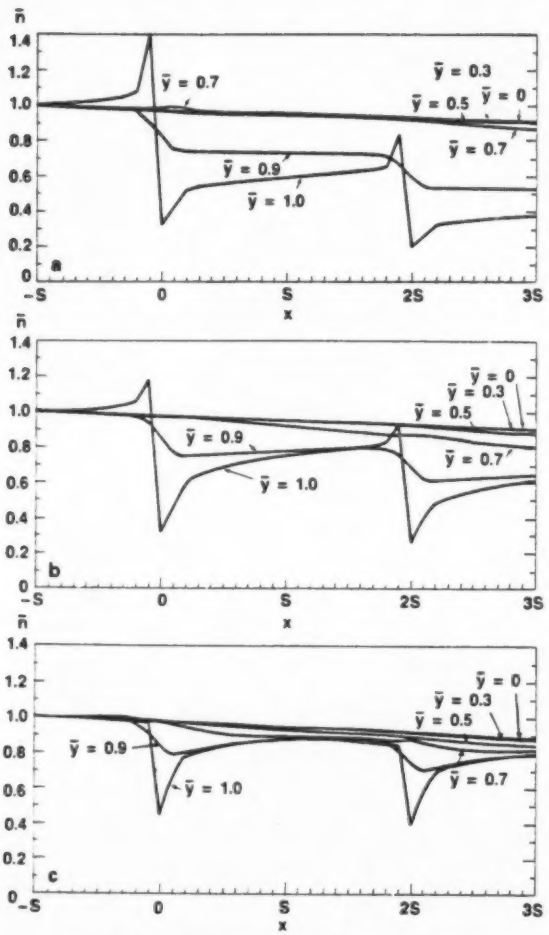

Fig. 6. Normalized particle concentration profiles for the wire-plate ESP; (a) $\epsilon^*=0.1$, $Pe=100$, $N_{EHD}=0$, $\eta=17.1\%$; (b) $\epsilon^*=0.1$, $Pe=10$, $N_{EHD}=0$, $\eta=17.0\%$; (c) $\epsilon^*=0.1$, $Pe=2$, $N_{EHD}=0$, $\eta=11.6\%$.

faster as a result of higher turbulent diffusion. When the flow becomes highly turbulent ($Pe=2$ or $D=1.83\times10^{-3}\,cm^2/s$), the concentration peak essentially disappears, as shown in Fig. 6c, and the concentration profile becomes uniform due to strong turbulent diffusion at the ESP outlet.

When the EHD effect is taken into account ($N_{EHD}=1.34$ or $y_m=0.2d$), the particle concentration profile for $Pe=100$ (or $D=0.37\times10^{-4}\,m^2/s$) and $\epsilon^*=0.1$ are shown in Fig. 7a. As can be seen from the figure, the concentration profile

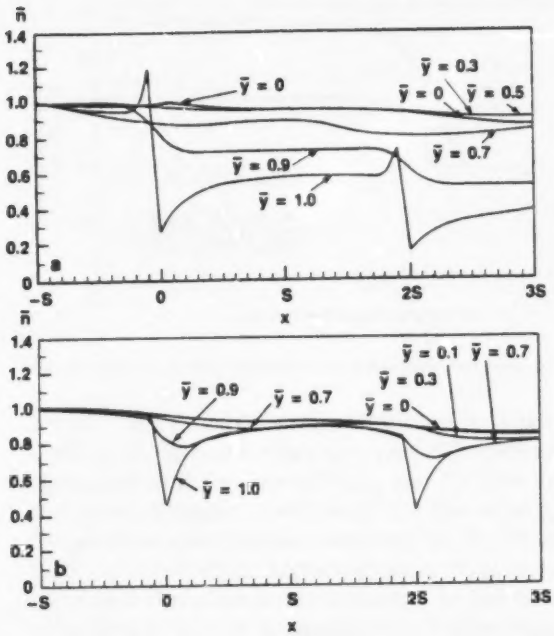

Fig. 7. Normalized particle concentration profiles for the wire-plate ESP; (a) $\epsilon^* = 0.1$, $Pe = 100$, $N_{EHD} = 1.34$, $\eta = 16.4\%$; (b) $\epsilon^* = 0.1$, $Pe = 2$, $N_{EHD} = 1.34$, $\eta = 16.6\%$.

becomes more wavy in the x-direction compared to the non-EHD case (Fig. 6a). The concentration peak becomes smaller because the primary velocity increases due to the secondary flow when approaching the wire electrode. As the turbulence further increases ($Pe = 2$, or $D = 0.18 \times 10^{-2}\ m^2/s$), the concentration profile becomes uniform and similar to the non-EHD case shown in Fig. 6c. This indicates that the turbulence dominates over the EHD or, in other words, the EHD effect disappears at high turbulence.

It should be noted that the diffusion approach, which includes the effect of the negative particle migration due to the concentration gradient, results in uniform concentration at high turbulence. As the value of D approaches infinity, the particle diffusion cancels out the particle migration, resulting in extremely low collection efficiency. On the other hand, the Deutsch assumption, which should be distinguished from the diffusion approach, simply assumes uniform concentration throughout the channel. Therefore, the collection efficiency is expected to be lower using the diffusion approach with high turbulence than that determined with the Deutsch assumption.

Figure 8 shows the fractional collection efficiency for the wire–plate ESP and plate–plate ESP. In the case of the wire–plate ESP, for values of D below

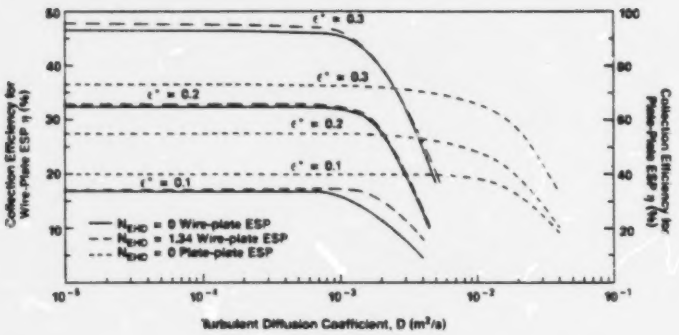
Collection Efficiency for Wire-Plate ESP η (%)
Collection Efficiency for Plate-Plate ESP η (%)
Turbulent Diffusion Coefficient, D (m²/s)
ε* = 0.3
ε* = 0.2
ε* = 0.1
N_EHD = 0 Wire-plate ESP
N_EHD = 1.34 Wire-plate ESP
N_EHD = 0 Plate-plate ESP

Fig. 8. Collection efficiency for both wire-plate and plate-plate ESPs.

1×10^{-3} m^2/s, the collection efficiency, η, is not affected by any turbulence or EHD level. However, when the value of D exceeds 1×10^{-3} m^2/s, η drops sharply regardless of the values of N_{EHD} and ϵ^*. This value of D is called "the critical turbulent diffusion coefficient" for the wire-plate ESP. Because numerical instabilities have been encountered for low Pe numbers (high turbulence), the higher η obtained for higher values of N_{EHD} may well be within the numerical error and therefore is inconclusive. In the case of the plate-plate ESP, the collection efficiency is significantly higher than for the wire-plate ESP. The critical turbulent diffusion coefficient increases to approximately 5×10^{-3} m^2/s. This indicates that η of the plate-plate ESP is less sensitive to the turbulence compared to that of the wire-plate ESP. It is also noted that η does not increase linearly with increasing ϵ^*.

The role of the EHD is to generate their circulatory cell near the plate and also to increase the turbulence, which is especially significant for the negative corona. It is clear from the present study that one of the most important considerations in designing the ESP is to reduce the turbulence level to less than the critical turbulent diffusion coefficient, so that the collection efficiency is dependent on particle migration and independent of turbulent or EHD effects.

References

1 G.L. Leonard, M. Mitchner and S.A. Self, Experimental study of the effect of turbulent diffusion on precipitator efficiency, J. Aerosol Sci., 13 (1982) 271-284.

2 K.D. Kihm, M. Mitchner and S.A. Self, Comparison of wire-plate and plate-plate electrostatic precipitators in turbulent flow, HTGL Report No. J-8, High Temperature Gasdynamics Laboratory, Mechanical Engineering Department, Stanford University, Stanford, CA, March 1985.

3 T. Yamamoto and L.E. Sparks, Effect of turbulent electrohydrodynamics on electrostatic precipitator efficiency, in: AIAA/ASME Fourth Fluid Mechanics, Gas Solid Flows, Plasma Dynamics and Lasers Conference, Atlanta, GA, May 1986, Vol. 35, pp. 35-39.

4 T. Yamamoto and H.R. Velkoff, Electrohydrodynamics in an electrostatic precipitator, J. Fluid Mech., 108 (1981) 1-18.

5 T. Yamamoto and L.E. Sparks, Numerical simulation of three-dimensional tuft corona and electrohydrodynamics, IEEE Trans. Ind. Appl., IA-22(5) (September/October 1986) 880-885.

6 T. Yamamoto, S. Nakamura and H.R. Velkoff, Numerical study of secondary flow interaction in an electrostatic precipitator, in: Innovative Numerical Analysis for Applied Engineering Science, University Press of Virginia, Charlottesville, VA, 1980, pp. 3-12.

NOTICE

This document has been reviewed in accordance with U.S. Environmental Protection Agency policy and approved for publication. Mention of trade names or commercial products does not constitute endorsement or recommendation for use.

This article documents research that was conducted under the auspices of the U.S. Environmental Protection Agency (USEPA). As an arm of the government, the USEPA has a paid up, non-exclusive, irrevocable, worldwide license to reproduce, prepare derivative works, and distribute to the public all of the material contained herein, and to grant others acting on its behalf the right to do so. The USEPA grants to the National Technical Information Service, Department of Commerce, the right to act as its agent in the distribution of this material.